Surface temperature and the dynamics of H2 on Cu(111)

Smits, B.

Chapter 4

Quantum dynamical surface temperature effects on the dissociative chemisorption of H_2 from Cu(111)

This chapter is based on Smits, B.; Litjens, L. G. B.; Somers, M. F. Accurate Description of the Quantum Dynamical Surface Temperature Effects on the Dissociative Chemisorption of H_2 from Cu(111). *The Journal of Chemical Physics* **2022**, *156*, 214706, DOI: 10.1063/5.0094985

Abstract

Accurately describing surface temperature effects for the dissociative scattering of H_2 on a metal surface at a quantum dynamical level is currently one of the open challenges for theoretical surface scientists. We present the first quantum dynamical (QD) simulations of hydrogen dissociating on a Cu(111) surface which accurately describe all relevant surface temperature effects, using the static corrugation model (SCM). The reaction probabilities we obtain show very good agreement with those found using quasi-classical dynamics (QCD) both for individual surface slabs and for an averaged, thus Monte-Carlo sampled, set of thermally distorted surface configurations. Rovibrationally elastic scattering probabilities show a much clearer difference between the QCD and QD results, which appears to be traceable back towards thermally distorted surface configurations with very low dissociation probabilities. This underlines the importance of investigating more observables than just dissociation. By

reducing the number of distorted surface atoms included in the dynamical model, we also show that only including one, or even three, surface atoms is generally not enough to accurately describe the effects of surface temperature on dissociation and elastic scattering. These results are a major step forward in accurately describing hydrogen scattering from a thermally excited Cu(111) surface. They open up a pathway to better describe reaction and scattering from other relevant crystal facets, such as stepped surfaces, at moderately elevated surface temperatures where quantum effects are expected to play a more important role in the dissociation of H_2 on Cu.

4.1 Introduction

One of the major focuses in the field of theoretical heterogeneous catalysis simulations is the accurate description of surface temperature effects on gas-solid reactive scattering[1–13]. These are especially of interest as they form an important basis for many industrial processes, such as the Haber-Bosch process [14] or H_2 powered engines[15]. To gain the most accurate description, these processes are broken down into their elementary steps, and a focus is put on describing each step individually.

In the past one often relied on the Born-Oppenheimer static surface (BOSS) approximation, where the surface is assumed to be both fully static and with the atoms in their ideal lattice positions, and electron and nucleus dynamics assumed to be fully separable[1]. Dynamics is performed using a 6D potential energy surface (PES) where all H_2 degrees of freedom are included, which is fit to density functional theory (DFT) results using i.e. the corrugation reducing procedure (CRP)[16]. These fitting procedures, however, often cannot or do not take into account the distorted nature of a thermally excited surface, while the relevant industrial processes, and experimental studies, are performed at elevated surface temperatures.

Nevertheless, some approaches do exist that can take these surface effects into account. These include a variety of methods including static distortion models and phonon baths studied by Busnengo *et al.*, and Jackson *et al.* for the CH_4 dissociation reaction [5, 7, 9–11, 17, 18]. Other approaches include the static disorder parameter by Manson and co-workers[19], the effective Hartree potential by Dutta *et al.*[12, 20], as well as the more general ring polymer molecular dynamics[21, 22] and high-dimensional neural network potential (HD-NNP) approaches[23–26].

HD-NNPs, in particular, are currently an intensively studied method to describing the PES, and have been shown to be usable in a wide variety of systems[23]. However, in our experience HD-NNPs also often still require

dense data sets, as extrapolation beyond the available dataset can yield wildly unexpected results. Careful planning in determining the appropriate symmetry functions[23]. While significant speed-ups can be achieved using these NNPs compared to AIMD simulations, we find they are generally not computationally fast enough to be used in state-of-the-art quantum dynamics (QD) simulations. Furthermore, none have yet been tested thoroughly by also computing accurate rotational and vibrational inelastic scattering or diffraction probabilities compared to experimental data[27–29]. As such, we believe HD-NNPs have not yet achieved the balance between speed and accuracy required for our application.

The system of choice in this thesis is the dissociative chemisorption of H_2 on a (thermally excited) Cu(111) surface, a particularly well studied model system, which would allow for a comparison to a wide range of both theoretical[3, 4, 8, 25, 30–34] and experimental [35–40] results. In particular, this system is being experimentally revisited by Alexandrowicz and co-workers, who have recently measured sharply defined state-to-state diffraction probabilities with their molecular interferometry setup[40–43]. Previous experimental work by Kaufmann *et al.* has also fully characterised a slow reaction channel of the H_2/Cu(111) system[39]. This reaction channel shows a strong temperature and vibrational dependency[37, 38], but has to our knowledge not yet been observed in theoretical studies.

Furthermore, using the specific reaction parameter (SRP) approach to DFT, Díaz *et al.* were already able to reproduce experimental molecular beam results to within 1 kcal / mol with the BOSS model[30]. The static corrugation model (SCM) further improved this BOSS model by adding an accurate description of surface temperature effects to quasi-classical dynamics (QCD) of H_2 dissociating on a Cu(111) surface[2]. The addition of a highly accurate embedded atom method (EAM) potential to generate thermally distorted surface slabs (Chapter 3) finally improved upon previous iterations of the SCM, which relied on random displacements to generate surface slabs[2, 3]. The introduction of the EAM potential also allowed for an explicit inclusion of surface motion into QCD using the dynamic corrugation model (DCM), as was shown in Chapter 3. Reaction and scattering probabilities obtained with this EAM-SCM and EAM-DCM show great agreement with experimental results and clearly demonstrated the validity of the sudden approximation for the H_2 on Cu(111) system.

Thus, the SCM is a prime candidate for introducing all relevant vibrational degrees of freedom into quantum dynamical simulations without also introducing a very large computational cost associated with introducing many more dynamical variables related to the surface atoms. Quantum effects are expected to be especially important for the description of accurate state-resolved

scattering probabilities, in particular for stepped surfaces such as Cu(211)[44]. Quantum effects are also expected to be important for an accurate description of (initially) rovibrationally excited H_2 molecules, or when considering lower surface temperatures (T_s). State-resolved scattering, rovibrationally excited molecules and lower surface temperatures are all important for describing industrial applications or reproducing experimental results. Potentials obtained using the SCM have also shown to be smooth enough to allow for an accurate description of both higher rovibrational states as well as state-resolved inelastic scattering probabilities[2–4]. However, the molecular dynamics used to generate surface slabs, as has been done using the EAM potential for $T_s = 925$ K, is not expected to yield accurate displacements for surface temperatures lower than 300 K[45].

The sudden approximation that lies at the basis of the SCM is expected to work best at a large mass mismatch between the reactant and the surface atom, and at shorter interaction times with the surface. However for those systems where the mass mismatch between H atoms and the transition metal atoms is very large, even the longer surface interaction times could likely be modeled accurately enough with a static surface. Electronic friction due to elecron-hole pair excitations is not included in our model as has been shown to not have a major effect for the H_2/Cu(111) system[46]. However, for other systems it might have to be included, which is currently only possible at a classical level[47–49].

In this Chapter, I present the use of the EAM-SCM to include all relevant surface temperature effects of the dissociation and rovibrationally elastic scattering of H_2 on a 925 K Cu(111) surface employing QD instead of QCD for the dynamics. First, the effect of constraining the H_2 molecule to a specific (1×1) unit cell using QCD will be discussed. Next, comparisons will be made between the reaction and elastic scattering probabilities obtained with QD and QCD, both for BOSS and EAM-SCM. For the EAM-SCM results, the probabilities curves are compared both for individual distorted slabs and as an average over all the slabs considered. This should shed light on the effect and importance of quantum effects, of H_2 and of the surface within a sudden approximation. Finally, the effect of displacing only a single or a limited number of surface atoms on the accurate description of the surface temperature effects is investigated.

4.2 Method

In this chapter, we will make use of the SCM as discussed in section 2.3.1 of Chapter 2 to describe the thermal surface effect of the H_2 chemisorption on

Cu(111), using both the QD TDWP approach as described in section 2.1.3 (QD-EAM-SCM) and the quasi-classical dynamics approach expanded upon in section 2.2.1 (QCD-EAM-SCM). The ideal lattice 6D PES that describes the perfect lattice surface interacting with the H_2 molecule is obtained from a corrugation reducing procedure (CRP) fit to density functional theory (DFT) results. This DFT dataset was obtained using the SRP48 exchange-correlation functional[8, 13]. The effective three-body coupling potential of the SCM, which expands the PES to include thermal lattice distortions, is also fitted to SRP48 DFT results[3]. Only those surface atoms within 16 bohrs ($\sim$ 8.47 Å) of the unit cell corner (U, V, Z)=(0, 0, 0) and within the top two layers of the distorted surface slab were included for the calculation of the SCM potential, as was done in the previous chapter.

4.2.1 Quantum dynamics

We obtain reaction and elastic scattering probabilities using QD for a total of 104 thermally distorted surface slabs. These slabs were acquired from unique traces of molecular dynamics using the EAM potential[45], as was described in Chapter 3. The reaction and scattering probabilities are averaged to get a single representative dissociation or elastic scattering probability curve of H_2 dissociating on, or scattering from, a thermally excited Cu(111) surface.

The reactive scattering of the H_2 is fast compared to the motion of the surface atoms, and the mass mismatch between the H and Cu atoms is very large. Thus, the hydrogen molecule and the solid represent two (thermally) separate systems, with the solid equilibrated to the surface temperature of 925 K, but the H_2 not. This would mean that the effects of the (quantum) dynamics of the surface on the reactive scattering of the H_2 can be (implicitly) included by using the sudden approximation. This is achieved by Monte-Carlo sampling many different surface degrees-of-freedom associated with the $\sim$70 surface atoms included in a typical SCM potential evaluation.

Compared to purely classical dynamics, the QD-SCM does not suffer from an incorrect redistribution of internal energies of both the solid and the hydrogen (especially when including a thermostat), or from erroneous use of Maxwell-Boltzmann statistics for the surface atoms at lower temperatures. The large amount of surface atoms that can be included with the SCM also provide a clear advantage over other approximate quantum dynamical studies, which generally make use of reduced degrees-of-freedom of the solid[33, 50], or describe the dynamics of the surface using a few Hartree products as anzats[12, 20]. Furthermore, with no need for a harmonic oscillator approximation for the

surface, the SCM allows for thermal expansion effects of the solid to be included, which have been shown to be clearly of relevance[2].

Evenmore, for the SCM and low surface temperatures, one could use the phonon displacement vectors to sample surface configurations with the correct Bose-Einstein statistics. Assuming one uses the proper periodic boundary conditions and the quasi-harmonic approximation[51]. This allows for a more direct comparison to earlier[52] and more recent state of the art diffraction experiments[40, 43] using a full quantum description of both H_2 and the solid, albeit within the sudden approximation where energy exchange is not taken into account.

For each individual surface configuration, the QD reaction or elastic scattering curve is obtained via three different wave packets, one with an energy range from 0.10 to 0.30 eV, 0.25−0.70 eV, and from 0.65−1.00 eV. Details regarding the computational parameters for each of these wave packets are described in the appendix (6.A) of Chapter 6.

4.2.2 Quasi-classical dynamics

These QD simulations fully including all relevant surface temperature effects are compared to QCD calculations. Surface atom displacements for the EAM-SCM approach are randomly selected from the total database of 25.000 surface configurations constructed in Chapter 3. Propagation is performed using the Bulirsch-Stoer predictor-corrector algorithm [53], ending when the two H atoms move more than 2.25 Å apart for a reactive trajectory, or when the Z c.m. coordinate is further than 7 Å from the surface for a scattered trajectory. For each incidence energy a total of 50.000 trajectories were performed, each using a unique surface configuration in the QCD-EAM-SCM. Additionally, each of the 104 surface configurations used in QD-EAM-SCM were also separately investigated with 50.000 trajectories per incidence energy using QCD-EAM-SCM.

In this chapter we also investigate the effect of applying a minimum image convention to the c.m. of the incoming H_2 molecule. When the c.m. moves further outside of the boundaries of 0 to a in both the lattice U and V coordinates, it is mapped back into the (1×1) unit cell when computing the PES and/or the forces associated with it. This makes the actual PES used in the dynamics to be translation symmetric when the molecule leaves the (1×1) unit cell. This translation symmetry constraint on the dynamics of H_2 is investigated in detail in order to verify the use of a single (1×1) unit cell in the QD. The SCM corrugation V_{coup} interaction could be influenced by such a symmetry constraint, as it is only diminished beyond approximately 10 bohrs /

5.5 Å (see the $P7$ parameter of Eq. 2.57)[3]. The use of a single (1×1) unit cell reduces the computational demands for the QD enormously. This is vital, as with the current approach to Monte-Carlo sample over at least 100 individual surfaces we present here entail a computationally challenging task, even when using the (1×1) single unit cell approximation.

4.2.3 Limited atom static corrugation model

In past works models to include surface atom degrees of freedom often focused primarily on distorting one, or a few, of the degrees of freedom (DoF) of the surface atom closest to the reactant impact site[10, 11, 33, 34, 54]. To investigate the quality of such an assumption for our system, we aim to also investigate the effect of only including a small number of surface atoms on the reaction and elastic scattering probabilities obtained using the EAM-SCM. Instead of using all atoms found within the 16 bohrs (∼ 8.47 Å) SCM cutoff radius described earlier in the methods section, distorted surface atoms are ranked based on their distance from the middle of the top layer of the (1×1) unit cell [(U, V, Z)=($\frac{a}{2}$, $\frac{a}{2}$, 0)]. Only a limited number of surface atoms are then included in the model, while all others are kept at their ideal lattice positions. This procedure allows us to easily navigate the approximations one makes if including only a limited number of surface DoFs at both the QCD as well as the QD level of theory. This method we will refer to as the limited atom SCM, or NAt-EAM-SCM. Here N stands for the number of surface atoms included, in this work 1At, 3At and 5At, for one, three and five surface atoms respectively.

4.3 Results and discussion

By comparing results from QD and QCD simulations of the dissociative chemisorption of H_2 on Cu(111), we aim to verify the quality of the SCM approach to including surface temperature effects into the QD simulations of the hydrogen molecule. Our focus will be on the rovibrational ground state of H_2, in particular comparing the results obtained using the QD-EAM-SCM and QCD-EAM-SCM approaches. The QD-EAM-SCM implements the QD of H_2 directly and fully correlated, but as stated before, the QD of the surface atom degrees of freedom are treated on a sudden approximation level using Monte-Carlo sampling. The QCD-EAM-SCM uses QCD for the dynamics of H_2 and again treats the dynamics of the surface on the same sudden approximation level, but with many more unique surface samples included compared to QD-EAM-SCM. In Chapter 3, the QCD-EAM-SCM was also validated (for D_2) to the DCM, where the surface was allowed to move. It was found that

the energy exchange possible in the DCM, but not in the SCM, was negligible (for D_2, which as a higher mass than H_2). We are therefore confident that the sudden approximation of the SCM for H_2 will hold even better, and allow us to perform the QD-EAM-SCM, via Monte-Carlo sampling, on such a scale.

The surface configurations we use in this EAM-SCM approach, both for the QCD and QD, were obtained from classical dynamics using the EAM potential at a modeled surface temperature of 925 K. This surface temperature was chosen to be able to compare to experimental results [32, 36], but is also well within the classical regime for this Cu system. This implies the correct use of the Maxwell-Boltzmann statistics, inherent to molecular dynamics, in the effective Monte-Carlo sampling in both QCD-EAM-SCM and QD-EAM-SCM.

4.3.1 Constrained results

One of the main constraints of our QD implementation is the size of the unit cell that can feasibly be used in the time-dependent wave packet (TDWP) method. Moving from a (1×1) to a (2×2) unit cell would already increase computational costs by a factor of four. While a small unit cell can easily be used with the BOSS approach, due to the periodicity of the ideal surface lattice, the same can not be assumed when thermally distorting the lattice. Therefore, we first investigated the effect of constraining the H_2 molecule to a (1×1) unit cell of the surface using, computationally much cheaper, QCD simulations. This translation symmetry constraint was simply implemented by always mapping the H_2 c.m. U and V coordinates into the single (1×1) unit cell before calculating the actual PES and the forces derived from it.

In Figure 4.1, we show the reaction and elastic scattering probabilities obtained with QCD for the H_2 on a Cu(111) surface at a modeled surface temperature of 925 K. Included are both the (1×1) unit cell constrained (1×1)-EAM-SCM and the unconstrained EAM-SCM results, for the (a) rovibrational ground state as well as a (b) vibrationally, (c) rotationally, and (d) rovibrationally excited initial state. Agreement between the constrained and non-constrained EAM-SCM results seems perfect for all four rovibrational states included, both for the reaction and elastic scattering probabilities. This excellent agreement confirms that the SCM does still yield accurate results when the H_2 molecule is constrained within a (1×1) unit cell of the surface for QCD, and likely also for QD.

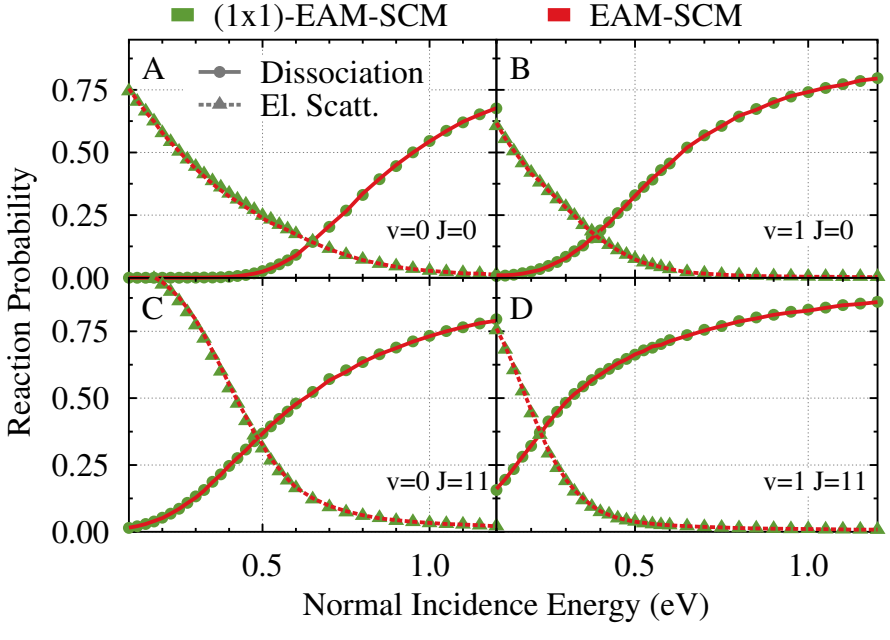

FIGURE 4.1: Reaction and rovibrationally elastic scattering probabilities obtained using both the (1×1)-EAM-SCM (green circles) and regular EAM-SCM (red curves). Reaction is shown as solid circles and lines, while the elastic scattering is shown as triangles and dashed lines. Included are: (a) the rovibrational ground state v = 0, J = 0; (b) a vibrationally excited state v = 1, J = 0; (c) a rotationally excited state v = 0, J = 11; and (d) a rovibrationally excited state v = 1, J = 11. The system of choice is H_2 reacting on a thermally distorted Cu(111) surface at a modeled surface temperature of 925 K.

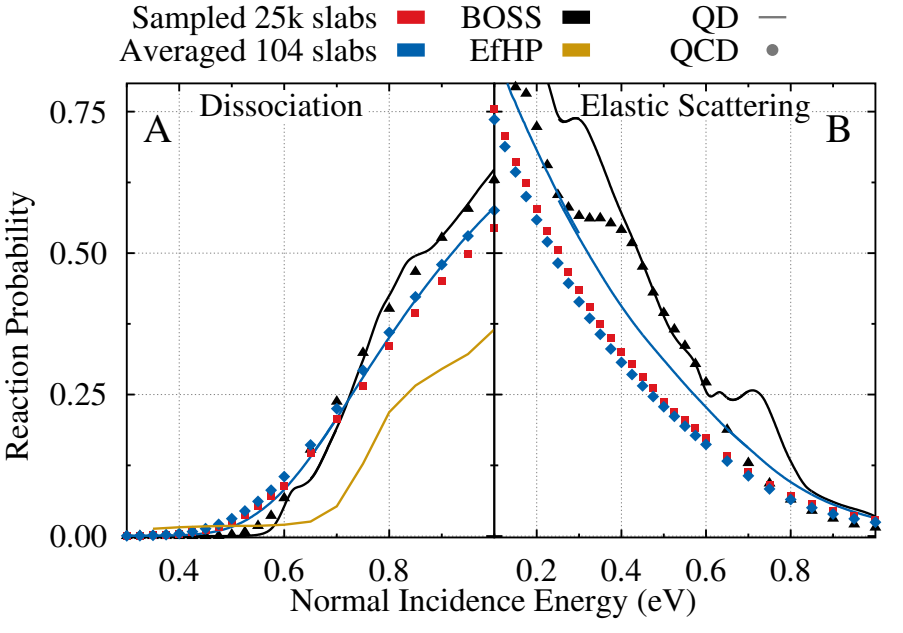

FIGURE 4.2: Reaction (a) and rovibrationally elastic scattering (b) probability curves for the H_2 in the rovibrational ground state (v = 0, J = 0) on a Cu(111) surface. Included are results obtained using the EAM-SCM both for a random sampling over all 25000 surface slabs with QCD (red squares), and an average of 104 selected surface slabs using both QD (blue curve) and QCD (blue diamonds). BOSS results for QD and QCD are shown as a black curve and black triangles, respectively. Finally reaction probabilities from other work by Adhikari *et al*, obtained using the QD EfHP approach[12], are shown as a yellow curve. For the EAM-SCM and EfHP results, a modeled surface temperature of 925 K is used.

4.3.2 Dissociative chemisorption and rovibrationally elastic scattering

With confirmation that the SCM still yields accurate results for H_2 constrained to a small (1×1) unit cell, we next include the EAM-SCM into our QD calculations. In Figure 4.2, we display the reaction (a) and rovibrationally elastic scattering (b) probability curves for the QD-EAM-SCM model, obtained as an average of calculations on 104 unique EAM generated surface slabs at a modeled surface temperature of 925 K. QCD-EAM-SCM results, obtained as an average of these 104 surface slabs, are also included. These results are also compared to QCD-EAM-SCM results obtained from randomly selecting surfaces out of the 25000 surface slabs available, as was done in Chapter 3. This allows us to get an estimate on the error we can expect when only including such a relatively low amount of unique surface slabs into our QD-EAM-SCM model. Furthermore, we also compare our results to those obtained by Dutta *et al.*, who applied their EfHP method to include thermal surface displacements into QD simulations for the same H_2/Cu(111) system[12]. They also used the same underlying BOSS CRP PES and SCM V_{coup} potentials, all based on the same SRP48 DFT functional, and exactly the same TDWP code. Finally, we also include results obtained using the perfect lattice BOSS approach both with QD and QCD, as has often been investigated in the past.

As expected, each dissociation probability curve shows a slow build-up at low incidence energy as most incoming adsorbates do not have enough energy to pass over the reaction barrier. At higher incidence energies, we find a mostly linear relation between the incidence energy and reaction, which will then eventually level off to a saturation value at energies well out of the plotted range. Only the QD-BOSS results show a slight deviation in this analysis, with a small "bump" in reaction probability around a normal incidence energy of 0.7 eV. The EfHP results displays by far the lowest reactivity, which can be explained by this model only including thermal displacements and not lattice expansion, as well as making other approximations related to the effective Hartree approach[2, 12]. Agreement between the reaction probabilities obtained for the 104 surface slabs compared to the results for a random selection of 25.000 surface slabs for QCD-EAM-SCM is good. This implies only a small error is expected in our QD-EAM-SCM results due to the relatively few surface slabs used. However some small variation is observed, indicating better results could be obtained if the number of included surface slabs is increased. Clearly this is possible at the expense of using more computational resources by simply running more TDWP QD runs. We have chosen, in view of the limited time, for using ∼100 surfaces for the QD-EAM-SCM and by estimating the error by

simply comparing to QCD-EAM-SCM results.

The QCD-EAM-SCM and the QD-EAM-SCM results show a much earlier curve onset, while also not increasing as steeply towards their maximum value, when compared to BOSS curves. This broadening of the reaction probability curve is generally associated with surface temperature effects, which we also show in Chapter 3 for the D_2/Cu(111) system, and is discussed in previous work[2, 32, 55]. Furthermore, the agreement between the QCD-EAM-SCM and QD-EAM-SCM results is also very good, with the QD curve displaying slightly less broadening. This is a strong indication of an accurate description of thermal surface effects in our QD results. However, this agreement is not perfect and thus also demonstrates subtle quantum effects do already come into play for the reaction of hydrogen on a 925 K copper surface.

When we consider the elastic scattering in Figure 4.2(b), we observe much less subtle quantum effects. Again the agreement between the scattering probabilities obtained for the 104 surface slabs compared to the results for a random selection of 25000 surface slabs for QCD-EAM-SCM is good. The BOSS results show some variation between QCD and QD, although this can be mostly attributed to the "bumps" we see around 0.3 and 0.7 eV, which we previously also showed for D_2 in Chapter 3.

A clear difference is visible when comparing the QD-EAM-SCM and QCD-EAM-SCM results, where QD shows a much higher probability for elastic scattering at lower incidence energies. This observation underlines the importance of properly investigating a system using QD, and shows the limited information available when only reaction probabilities are investigated and compared. Furthermore, these quantum effects could become even more important for higher initial rovibrational states of the H_2, especially for rovibrational inelastic scattering and/or diffraction. It is also expected to be especially important for lower surface temperatures or scattering reactions from stepped surfaces [Cu(211)]. Unfortunately, this has not been investigated thoroughly yet, partly due to the computational challenges associated with these systems.

However, the SCM approach (for H_2 and D_2), and the use of the scattering amplitude formalism in the QD are expected to really shines here.

To further investigate the quality of the QD dynamics compared to our QCD results, we take a closer look at the reaction and elastic scattering results on a few individual thermally distorted surface slabs. Especially of interest are those surfaces where the dissociation probability is either much higher or lower than on average. This allows us to validate the model not just on average when Monte-Carlo sampling over many surface configurations, but also for the specific edge cases it will have to deal with.

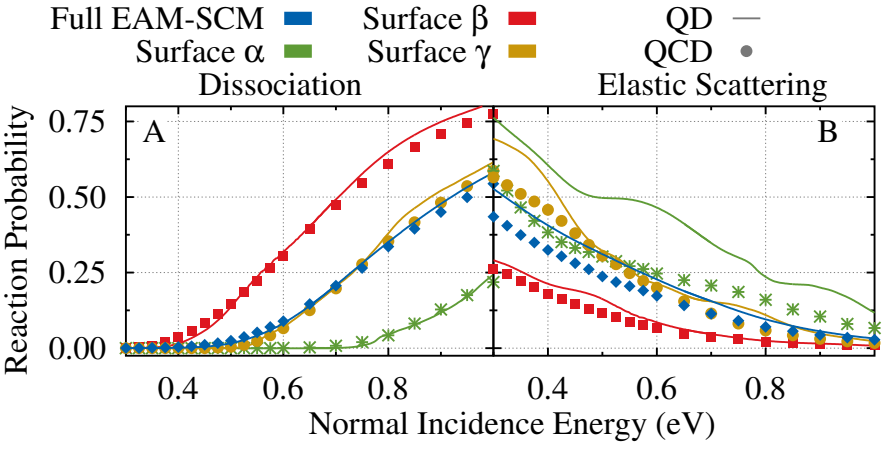

FIGURE 4.3: Reaction (a) and rovibrationally elastic scattering (b) probabilities for three specific thermally excited surface slabs, and the average of all investigated distorted surface slabs. A a modeled surface temperature of 925 K was used with the incident H_2 in the rovibrational ground state. Results for surface α, β, and γ are shown as green stars and curves, red squares and curves, and yellow circles and curves, respectively. The results for the averaged probabilities obtained using the EAM-SCM are shown as blue curves and diamonds. The curves represent the QD results, while the symbols represent the QCD results. For the full EAM-SCM results, the QD curves consist of an average of 104 surface slabs, while the QCD results are obtained from random sampling of all 25.000 distorted surface slabs.

In Figure 4.3(a), we show reaction probabilities for three different surface slabs: not very reactive (surface α), very reactive (surface β) and typical (surface γ). Also included are the averaged results for all the EAM-SCM distorted surface slabs.

For dissociation, we again see the characteristic S-curve shape, with the results for the more reactive surface slab β already levelling off towards a saturation value. In contrast, the curve the less reactive surface slab α just passed the curve onset and is reaching the linear part of the S-curve. Overall, the agreement between the QCD results as symbols and the QD results as a line is excellent. As was the case for the Monte-Carlo sampled results, we see a small decrease in curve broadness for QD compared to QCD, which is more visible for the results of slab β than for the other two.

In general, we see no great variation in the agreement between QCD and QD when we compare the reaction probabilities found for the individual surface slabs to those obtained for the general average. However, no such claim can be made for the elastic scattering probabilities, as can be seen in Figure 4.3(b). We find great agreement between the rovibrationally elastic scattering probabilities obtained using the reactive surface slab β, better than that of the averaged results. In contrast, the agreement between the QD and QCD probabilities found for the typical slab γ are close in line to that found for the full average of all surface slabs. Finally, the probabilities found for the less reactive surface slab α show the largest difference between the QD- and QCD-EAM-SCM. This appears to indicate that the differences between the QD and QCD elastic scattering probabilities we find in Figure 4.2(b). are primarily caused by those surface slabs that have a much higher barrier due to the thermal distortion of the surface. However, further studies, also including more surface slabs into the QD-EAM-SCM, will be required to fully understand this phenomenon.

4.3.3 Limited surface atom degrees of freedom

In previous studies, the effect of including surface atom degrees of freedom were often described through the displacement of a single surface atom, or even a single DoF of a single surface atom[10, 11, 33]. While such an approach is computationally very efficient, it is not too clear if all thermal surface effects can be described through such a small number of degrees of freedom, or even a single one. Using the EAM-SCM, we are able to selectively include or exclude the contribution of specific distorted surface atoms. With this, we aim to investigate the effect of reducing the number of surface atoms taken into account for the thermal surface effects of the H_2 on Cu(111) system, both in QD and QCD.

In Figure 4.4, we show the reaction and rovibrationally elastic scattering probabilities obtained with QD- and QCD-EAM-SCM when only including one, three or five thermally distorted Cu(111) surface atoms. The surface atoms to include were selected based on their distance from the center of the (1×1) Cu(111) surface unit cell, starting with the closest surface atom. Also included are the results of the full EAM-SCM model, which includes ∼70 surface atoms depending on the specific distorted surface slab used, and the BOSS results.

Again, agreement between reaction probabilities obtained QD-EAM-SCM and QCD-EAM-SCM appears to be very good, even for those results where less surface atoms are included in the model. We also see a clear decrease in elastic scattering probabilities obtained with QD-EAM-SCM compared to QCD-EAM-SCM for all the EAM-SCM results. However, there is also a clear difference between the EAM-SCM results where less surface atoms are taken into account, both for reaction and scattering probabilities. In particular, the scattering and dissociation curves show much more "BOSS-like" probabilities, with less of the broadening usually attributed to surface temperature effects, when only a single surface atom is thermally displaced. Adding two more surface atoms to the model already greatly increases agreement with the full EAM-SCM model, although there is still a noticeable discrepancy with the results obtained from the full model. Finally, the 5At-EAM-SCM results show excellent agreement with the full model This appears to indicate that correctly implementing surface temperature effects will require at least five surface atoms to be included to get accurate results for the H_2 on Cu(111) system when including a modeled surface temperature of 925 K. The observation that using only five surface atoms already gives such good results correlates with the effectiveness of only using a single (1×1) unit cell for the QD, as only ∼10 surface atoms are found within the ∼7 bohrs (∼3.7 Å) distance where V_{coup} contributes significantly towards the potential energy of the PES[3]. This is an important characteristic to keep in mind when designing new models for including surface temperature, although it is currently unclear if this characteristic is specific for our system, or even the model used to describe it.

4.4 Conclusion

We investigated the quality of the EAM-SCM in quantum dynamical calculations to accurately describe all relevant surface temperature effects. Dissociation and rovibrationally elastic scattering probabilities were computed, using both QCD and QD, for the H_2 on Cu(111) system at a modeled surface temperature of 925 K for the rovibrational ground state. Similar the previous chapter a CRP PES based on the SRP48 functional was used, which has been shown to be

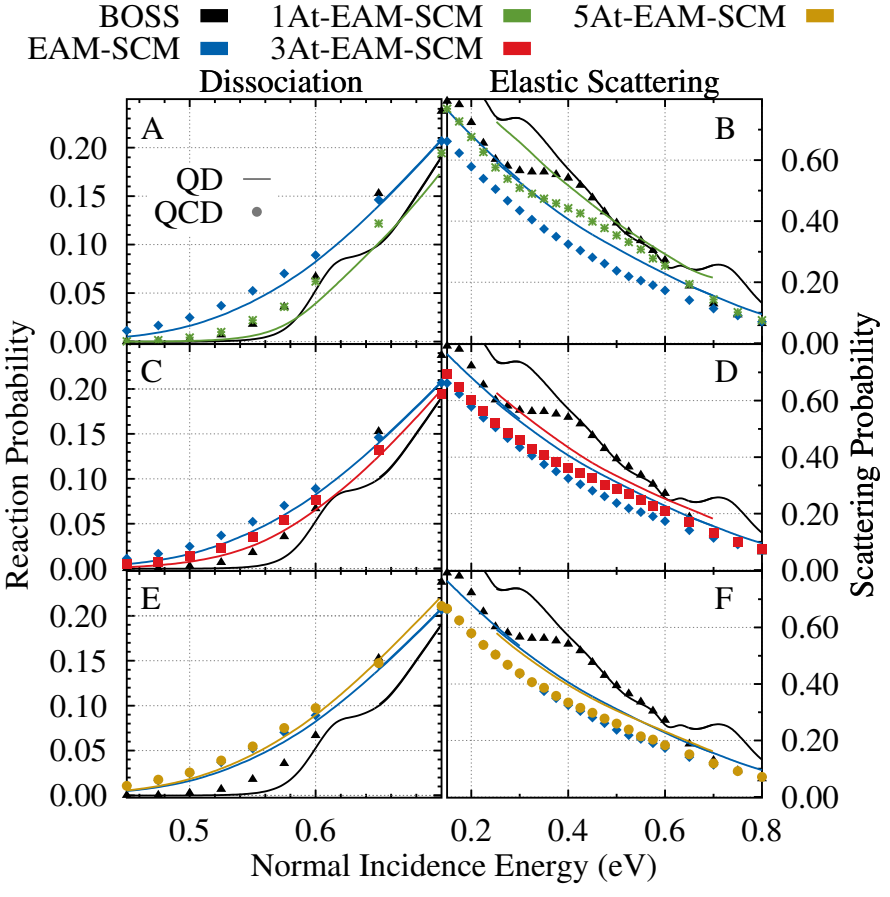

FIGURE 4.4: Reaction [(a), (c), and (e)] and rovibrationally elastic scattering [(b), (d), and (f)] probabilities obtained for the 1At-, 3At- and 5At-EAM-SCM approach, as well as the full EAM-SCM and the BOSS approaches. Here, 1At, 3At, and 5At refer to the number of surface atoms included into the EAM-SCM, and are shown as green stars and curves [(a) and (b)], as red squares and curves [(c) and (d)], and as yellow circles and curves [(e) and (f)], respectively. The BOSS results are included as black curves and triangles, and the full surface EAM-SCM results are shown as blue diamonds and curves. The curves represent the QD results, while the symbols represent the QCD results. The QD curves consist of an average of 104 surface slabs, for the EAM-SCM results with one, three, five, and all thermally distorted surface atoms (within the cutoff) included consist of an average of 104 surface slabs. The QCD results are obtained from random sampling of all 25.000 distorted surface slabs.

chemically accurate[30]. The SCM coupling potential was described using the effective three-body potential as published by Spiering *et al.*[3]. The surface configurations used were obtained with molecular dynamics using a highly accurate EAM potential[45], as is described in Chapter 3.

Before implementing the SCM into our QD calculations, we first investigated the effect of constraining the H_2 molecule to a (1×1) unit cell, as much larger cells are computationally unfeasible for QD. Reaction and elastic scattering probabilities obtained using QCD and a variety of rovibrational states showed excellent agreement between those simulations where the H_2 molecules were and were not constrained.

With confirmation that the SCM would yield accurate results, even when such a small unit cell is used, we next included the EAM-SCM into our quantum dynamics. Both the QCD and QD reaction probability curves obtained using the SCM showed the characteristic curve broadening compared to the BOSS results found when surface temperature effects are taken into account. Furthermore, the QCD- and QD-EAM-SCM results showed great agreement with each other when considering reaction probabilities, which indicates the quality of the quasi-classical approach for this system and observable. The QD-EAM-SCM results did display a very slight decrease in curve broadening compared to the QCD results, which clearly indicates a quantum effect that could be of importance. The QD-EAM-SCM elastic scattering probabilities were found to be significantly higher than the QCD results, which could indicate an important quantum effect for this system. In contrast, for the BOSS model the difference in scattering probability was much less apparent, which could indicate a role of surface temperature effects or our model in particular.

To further investigate this difference between QD and QCD, we next compared reaction and scattering probabilities obtained for several specific distorted surfaces using the EAM-SCM. A highly reactive, a less reactive, and a typical surface slab were chosen for comparison, to get an overview of the different types of surface slabs available. Again reaction probabilities were found to have great agreement between QD and QCD, even for the three specific surface slabs, although the highly reactive slab again displayed a small difference in curve broadness between QD-EAM-SCM and QCD-EAM-SCM. Interestingly, elastic scattering probabilities obtained for the typical and highly reactive surface configurations also showed great agreement between the QCD and QD results, whereas as clear difference between QCD and QD was found only for the less reactive surface configuration. This could indicate the difference in elastic scattering probabilities found is primarily caused by those surfaces that show a low reactivity, although further work would be required to fully investigate this finding.

Finally, we aimed at getting a better understanding of surface atom degrees of freedom that play a relevant role in describing the surface temperature effects with the SCM approach. Reaction and elastic scattering probabilities were obtained using EAM-SCM where only one, three or five surface atoms where thermally displaced. These probabilities were then compared to those obtained using both the BOSS model and the full EAM-SCM. We found that including the thermal distortions of only one surface atom into the system was not sufficient to accurately describing the surface temperature effects of the system, with this approach more closely resembling the BOSS results than the EAM-SCM results. Only when a total of five surface atom degrees of freedom were included in the model did we find close to an accurate description of the thermally distorted surface. A clear difference was already found between the elastic scattering probabilities obtained using QD and QCD even for those curves where only a single distorted surface was included in the EAM-SCM, however.

Previous work has already shown that the underlying DFT functional of V_{coup} is transferable between different facets of the copper surface[44, 56]. This opens up the opportunity to expand this work further towards the Cu(100) facet and eventually the Cu(211) stepped surface. However, the number of surface slabs in the Monte-Carlo sampling in this work were quite limited (104), and as such we expect to obtain more definitive results once more QD-EAM-SCM simulations can be performed, also including results from different initial rovibrational states of H_2. Additional work is also required to allow for accurate results of reactive scattering from surface slabs below approximately 300 K[45]. Here the classical MD approach to generating slabs with the EAM is expected not to give accurate results, predominantly because the use of a thermostat that extracts the zero point energy from the Cu system, but also from implicitly employing a Maxwell-Boltzmann statistical sampling of the phonons that are actually bosons and adhere to the Bose-Einstein statistics[12].

References

(1) Kroes, G.-J.; Díaz, C. Quantum and classical dynamics of reactive scattering of H_2 from metal surfaces. *Chemical Society Reviews* **2016**, *45*, 3658–3700, DOI: 10.1039/c5cs00336a.

(2) Wijzenbroek, M.; Somers, M. F. Static surface temperature effects on the dissociation of H_2 and D_2 on Cu(111). *The Journal of Chemical Physics* **2012**, *137*, 054703, DOI: 10.1063/1.4738956.

(3) Spiering, P.; Wijzenbroek, M.; Somers, M. F. An improved static corrugation model. *The Journal of Chemical Physics* **2018**, *149*, 234702, DOI: 10.1063/1.5058271.

(4) Smits, B.; Somers, M. F. Beyond the static corrugation model: Dynamic surfaces with the embedded atom method. *The Journal of Chemical Physics* **2021**, *154*, 074710, DOI: 10.1063/5.0036611.

(5) Jackson, B. Quantum studies of methane-metal inelastic diffraction and trapping: The variation with molecular orientation and phonon coupling. *Chemical Physics* **2022**, *559*, 111516, DOI: 10.1016/j.chemphys.2022.111516.

(6) Kroes, G.-J. Computational approaches to dissociative chemisorption on metals: towards chemical accuracy. *Physical Chemistry Chemical Physics* **2021**, *23*, 8962–9048, DOI: 10.1039/D1CP00044F.

(7) Xiao, Y.; Dong, W.; Busnengo, H. F. Reactive force fields for surface chemical reactions: A case study with hydrogen dissociation on Pd surfaces. *The Journal of Chemical Physics* **2010**, *132*, 014704, DOI: 10.1063/1.3265854.

(8) Mondal, A.; Wijzenbroek, M.; Bonfanti, M.; Díaz, C.; Kroes, G.-J. Thermal Lattice Expansion Effect on Reactive Scattering of H_2 from Cu(111) at $T_s = 925$ K. *The Journal of Physical Chemistry A* **2013**, *117*, 8770–8781, DOI: 10.1021/jp4042183.

(9) Seminara, G. N.; Peludhero, I. F.; Dong, W.; Martínez, A. E.; Busnengo, H. F. Molecular Dynamics Study of Molecular and Dissociative Adsorption Using System-Specific Force Fields Based on Ab Initio Calculations: CO/Cu(110) and CH_4/Pt(110). *Topics in Catalysis* **2019**, *62*, 1044–1052, DOI: 10.1007/s11244-019-01196-9.

(10) Tiwari, A. K.; Nave, S.; Jackson, B. The temperature dependence of methane dissociation on Ni(111) and Pt(111): Mixed quantum-classical studies of the lattice response. *The Journal of Chemical Physics* **2010**, *132*, 134702, DOI: 10.1063/1.3357415.

(11) Guo, H.; Farjamnia, A.; Jackson, B. Effects of Lattice Motion on Dissociative Chemisorption: Toward a Rigorous Comparison of Theory with Molecular Beam Experiments. *The Journal of Physical Chemistry Letters* **2016**, *7*, 4576–4584, DOI: 10.1021/acs.jpclett.6b01948.

(12) Dutta, J.; Mandal, S.; Adhikari, S.; Spiering, P.; Meyer, J.; Somers, M. F. Effect of surface temperature on quantum dynamics of H_2 on Cu(111) using a chemically accurate potential energy surface. *The Journal of Chemical Physics* **2021**, *154*, 104103, DOI: 10.1063/5.0035830.

(13) Nattino, F.; Díaz, C.; Jackson, B.; Kroes, G.-J. Effect of Surface Motion on the Rotational Quadrupole Alignment Parameter of D_2 Reacting on Cu(111). *Physical Review Letters* **2012**, *108*, 236104, DOI: 10.1103/PhysRevLett.108.236104.

(14) Smith, C.; Hill, A. K.; Torrente-Murciano, L. Current and future role of Haber–Bosch ammonia in a carbon-free energy landscape. *Energy & Environmental Science* **2020**, *13*, 331–344, DOI: 10.1039/C9EE02873K.

(15) Zambelli, T.; Barth, J. V.; Wintterlin, J.; Ertl, G. Complex pathways in dissociative adsorption of oxygen on platinum. *Nature* **1997**, *390*, 495–497, DOI: 10.1038/37329.

(16) Busnengo, H. F.; Salin, A.; Dong, W. Representation of the 6D potential energy surface for a diatomic molecule near a solid surface. *The Journal of Chemical Physics* **2000**, *112*, 7641–7651, DOI: 10.1063/1.481377.

(17) Lozano, A.; Shen, X. J.; Moiraghi, R.; Dong, W.; Busnengo, H. F. Cutting a chemical bond with demon's scissors: Mode- and bond-selective reactivity of methane on metal surfaces. *Surface Science* **2015**, *640*, 25–35, DOI: 10.1016/j.susc.2015.04.002.

(18) Jackson, B. The Trapping of Methane on Ir(111): A First-Principles Quantum Study. *The Journal of Chemical Physics* **2021**, *155*, 044705, DOI: 10.1063/5.0058672.

(19) Kroes, G. J.; Wijzenbroek, M.; Manson, J. R. Possible effect of static surface disorder on diffractive scattering of H_2 from Ru(0001): Comparison between theory and experiment. *The Journal of Chemical Physics* **2017**, *147*, 244705, DOI: 10.1063/1.5011741.

(20) Dutta, J.; Naskar, K.; Adhikari, S.; Spiering, P.; Meyer, J.; Somers, M. F. Effect of surface temperature on quantum dynamics of D_2 on Cu(111) using a chemically accurate potential energy surface, To Be Submitted, 2022, submitted.

(21) Craig, I. R.; Manolopoulos, D. E. Quantum Statistics and Classical Mechanics: Real Time Correlation Functions from Ring Polymer Molecular Dynamics. *The Journal of Chemical Physics* **2004**, *121*, 3368–3373, DOI: 10.1063/1.1777575.

(22) Suleimanov, Y. V.; Aoiz, F. J.; Guo, H. Chemical Reaction Rate Coefficients from Ring Polymer Molecular Dynamics: Theory and Practical Applications. *The Journal of Physical Chemistry A* **2016**, *120*, 8488–8502, DOI: 10.1021/acs.jpca.6b07140.

(23) Behler, J. First Principles Neural Network Potentials for Reactive Simulations of Large Molecular and Condensed Systems. *Angewandte Chemie International Edition* **2017**, *56*, 12828–12840, DOI: https://doi.org/10.1002/anie.201703114.

(24) Artrith, N.; Behler, J. High-dimensional neural network potentials for metal surfaces: A prototype study for copper. *Physical Review B* **2012**, *85*, 045439, DOI: 10.1103/PhysRevB.85.045439.

(25) Zhu, L.; Zhang, Y.; Zhang, L.; Zhou, X.; Jiang, B. Unified and transferable description of dynamics of H_2 dissociative adsorption on multiple copper surfaces *via* machine learning. *Physical Chemistry Chemical Physics* **2020**, *22*, 13958–13964, DOI: 10.1039/D0CP02291H.

(26) Lin, Q.; Zhang, L.; Zhang, Y.; Jiang, B. Searching Configurations in Uncertainty Space: Active Learning of High-Dimensional Neural Network Reactive Potentials. *Journal of Chemical Theory and Computation* **2021**, *17*, 2691–2701, DOI: 10.1021/acs.jctc.1c00166.

(27) Somers, M. F.; Olsen, R. A.; Busnengo, H. F.; Baerends, E. J.; Kroes, G. J. Reactive scattering of H_2 from Cu(100): Six-dimensional quantum dynamics results for reaction and scattering obtained with a new, accurately fitted potential-energy surface. *The Journal of Chemical Physics* **2004**, *121*, 11379–11387, DOI: 10.1063/1.1812743.

(28) Cueto, M. d.; Muzas, A. S.; Somers, M. F.; Kroes, G. J.; Díaz, C.; Martín, F. Exploring surface landscapes with molecules: rotationally induced diffraction of H_2 on LiF(001) under fast grazing incidence conditions. *Physical Chemistry Chemical Physics* **2017**, *19*, 16317–16322, DOI: 10.1039/C7CP02904G.

(29) Muzas, A. S.; del Cueto, M.; Gatti, F.; Somers, M. F.; Kroes, G. J.; Martín, F.; Díaz, C. H_2LiF(001) diffractive scattering under fast grazing incidence using a DFT-based potential energy surface. *Physical Review B* **2017**, *96*, 205432, DOI: 10.1103/PhysRevB.96.205432.

(30) Díaz, C.; Pijper, E.; Olsen, R. A.; Busnengo, H. F.; Auerbach, D. J.; Kroes, G. J. Chemically accurate simulation of a prototypical surface reaction: H_2 dissociation on Cu(111). *Science (New York, N.Y.)* **2009**, *326*, 832–834, DOI: 10.1126/science.1178722.

(31) Díaz, C.; Olsen, R. A.; Auerbach, D. J.; Kroes, G. J. Six-Dimensional Dynamics Study of Reactive and Non Reactive Scattering of H_2 from Cu(111) Using a Chemically Accurate Potential Energy Surface. *Physical Chemistry Chemical Physics* **2010**, *12*, 6499–6519, DOI: 10.1039/C001956A.

(32) Nattino, F.; Genova, A.; Guijt, M.; Muzas, A. S.; Díaz, C.; Auerbach, D. J.; Kroes, G.-J. Dissociation and recombination of D_2 on Cu(111): ab initio molecular dynamics calculations and improved analysis of desorption experiments. *The Journal of Chemical Physics* **2014**, *141*, 124705, DOI: 10.1063/1.4896058.

(33) Bonfanti, M.; Somers, M. F.; Díaz, C.; Busnengo, H. F.; Kroes, G.-J. 7D Quantum Dynamics of H_2 Scattering from Cu(111): The Accuracy of the Phonon Sudden Approximation. *Zeitschrift für Physikalische Chemie* **2013**, 130617035227002, DOI: 10.1524/zpch.2013.0405.

(34) Kroes, G.-J.; Juaristi, J. I.; Alducin, M. Vibrational Excitation of H_2 Scattering from Cu(111): Effects of Surface Temperature and of Allowing Energy Exchange with the Surface. *The Journal of Physical Chemistry C* **2017**, *121*, 13617–13633, DOI: 10.1021/acs.jpcc.7b01096.

(35) Michelsen, H. A.; Rettner, C. T.; Auerbach, D. J.; Zare, R. N. Effect of rotation on the translational and vibrational energy dependence of the dissociative adsorption of D_2 on Cu(111). *The Journal of Chemical Physics* **1993**, *98*, 8294–8307, DOI: 10.1063/1.464535.

(36) Rettner, C. T.; Michelsen, H. A.; Auerbach, D. J. Quantum-state-specific dynamics of the dissociative adsorption and associative desorption of H_2 at a Cu(111) surface. *The Journal of Chemical Physics* **1995**, *102*, 4625–4641, DOI: 10.1063/1.469511.

(37) Hou, H.; Gulding, S. J.; Rettner, C. T.; Wodtke, A. M.; Auerbach, D. J. The Stereodynamics of a Gas-Surface Reaction. *Science* **1997**, *277*, 80–82, DOI: 10.1126/science.277.5322.80.

(38) Murphy, M. J.; Hodgson, A. Adsorption and desorption dynamics of H_2 and D_2 on Cu(111): The role of surface temperature and evidence for corrugation of the dissociation barrier. *The Journal of Chemical Physics* **1998**, *108*, 4199–4211, DOI: 10.1063/1.475818.

(39) Kaufmann, S.; Shuai, Q.; Auerbach, D. J.; Schwarzer, D.; Wodtke, A. M. Associative desorption of hydrogen isotopologues from copper surfaces: Characterization of two reaction mechanisms. *The Journal of Chemical Physics* **2018**, *148*, 194703, DOI: 10.1063/1.5025666.

(40) Chadwick, H.; Somers, M. F.; Stewart, A. C.; Alkoby, Y.; Carter, T. J. D.; Butkovicova, D.; Alexandrowicz, G. Stopping Molecular Rotation Using Coherent Ultra-Low-Energy Magnetic Manipulations. *Nature Communications* **2022**, *13*, 2287, DOI: 10.1038/s41467-022-29830-3.

(41) Godsi, O.; Corem, G.; Alkoby, Y.; Cantin, J. T.; Krems, R. V.; Somers, M. F.; Meyer, J.; Kroes, G.-J.; Maniv, T.; Alexandrowicz, G. A general method for controlling and resolving rotational orientation of molecules in molecule-surface collisions. *Nature Communications* **2017**, *8*, 15357, DOI: 10.1038/ncomms15357.

(42) Alkoby, Y.; Chadwick, H.; Godsi, O.; Labiad, H.; Bergin, M.; Cantin, J. T.; Litvin, I.; Maniv, T.; Alexandrowicz, G. Setting benchmarks for modelling gas–surface interactions using coherent control of rotational orientation states. *Nature Communications* **2020**, *11*, 3110, DOI: 10.1038/s41467-020-16930-1.

(43) Chadwick, H.; Alkoby, Y.; Cantin, J. T.; Lindebaum, D.; Godsi, O.; Maniv, T.; Alexandrowicz, G. Molecular spin echoes; multiple magnetic coherences in molecule surface scattering experiments. *Physical Chemistry Chemical Physics* **2021**, *23*, 7673–7681, DOI: 10.1039/D0CP05399F.

(44) Smeets, E. W. F.; Füchsel, G.; Kroes, G.-J. Quantum Dynamics of Dissociative Chemisorption of H_2 on the Stepped Cu(211) Surface. *The Journal of Physical Chemistry C* **2019**, *123*, 23049–23063, DOI: 10.1021/acs.jpcc.9b06539.

(45) Sheng, H. W.; Kramer, M. J.; Cadien, A.; Fujita, T.; Chen, M. W. Highly optimized embedded-atom-method potentials for fourteen fcc metals. *Physical Review B* **2011**, *83*, 134118, DOI: 10.1103/PhysRevB.83.134118.

(46) Spiering, P.; Meyer, J. Testing Electronic Friction Models: Vibrational De-excitation in Scattering of H_2 and D_2 from Cu(111). *The Journal of Physical Chemistry Letters* **2018**, *9*, 1803–1808, DOI: 10.1021/acs.jpclett.7b03182.

(47) Füchsel, G.; Klamroth, T.; Monturet, S.; Saalfrank, P. Dissipative Dynamics within the Electronic Friction Approach: The Femtosecond Laser Desorption of H_2/D_2 from Ru(0001). *Physical Chemistry Chemical Physics* **2011**, *13*, 8659, DOI: 10.1039/c0cp02086a.

(48) Maurer, R. J.; Jiang, B.; Guo, H.; Tully, J. C. Mode Specific Electronic Friction in Dissociative Chemisorption on Metal Surfaces: H_2 on Ag(111). *Physical Review Letters* **2017**, *118*, 256001, DOI: 10.1103/PhysRevLett.118.256001.

(49) Spiering, P.; Shakouri, K.; Behler, J.; Kroes, G.-J.; Meyer, J. Orbital-Dependent Electronic Friction Significantly Affects the Description of Reactive Scattering of N_2 from Ru(0001). *The Journal of Physical Chemistry Letters* **2019**, *10*, 2957–2962, DOI: 10.1021/acs.jpclett.9b00523.

(50) Smits, B.; Litjens, L. G. B.; Somers, M. F. Accurate Description of the Quantum Dynamical Surface Temperature Effects on the Dissociative Chemisorption of H_2 from Cu(111). *The Journal of Chemical Physics* **2022**, *156*, 214706, DOI: 10.1063/5.0094985.

(51) Togo, A.; Tanaka, I. First Principles Phonon Calculations in Materials Science. *Scripta Materialia* **2015**, *108*, 1–5, DOI: 10.1016/j.scriptamat.2015.07.021.

(52) Farias, D.; Rieder, K.-H. Atomic Beam Diffraction from Solid Surfaces. *Reports on Progress in Physics* **1998**, *61*, 1575, DOI: 10.1088/0034-4885/61/12/001.

(53) Bulirsch, R.; Stoer, J. Numerical treatment of ordinary differential equations by extrapolation methods. *Numerische Mathematik* **1966**, *8*, 1–13, DOI: 10.1007/BF02165234.

(54) Busnengo, H. F.; Di Césare, M. A.; Dong, W.; Salin, A. Surface Temperature Effects in Dynamic Trapping Mediated Adsorption of Light Molecules on Metal Surfaces: H 2 on Pd(111) and Pd(110). *Physical Review B* **2005**, *72*, 125411, DOI: 10.1103/PhysRevB.72.125411.

(55) *Dynamics of Gas-Surface Interactions: Atomic-level Understanding of Scattering Processes at Surfaces*; Muino, R. D., Busnengo, H. F., Eds.; Springer Series in Surface Sciences; Springer-Verlag: Berlin Heidelberg, 2013, DOI: 10.1007/978-3-642-32955-5.

(56) Sementa, L.; Wijzenbroek, M.; van Kolck, B. J.; Somers, M. F.; Al-Halabi, A.; Busnengo, H. F.; Olsen, R. A.; Kroes, G. J.; Rutkowski, M.; Thewes, C.; Kleimeier, N. F.; Zacharias, H. Reactive scattering of H_2 from Cu(100): Comparison of dynamics calculations based on the specific reaction parameter approach to density functional theory with experiment. *The Journal of Chemical Physics* **2013**, *138*, 044708, DOI: 10.1063/1.4776224.